

Stable Haptic Teleoperation of UAVs via Small \mathcal{L}_2 Gain and Control Barrier Functions

Dawei Zhang¹, Roberto Tron²

Abstract—We present a novel haptic teleoperation approach that considers not only the safety but also the stability of a teleoperation system. Specifically, we build upon previous work on *haptic shared control*, which generates a reference haptic feedback that helps the human operator to safely navigate the robot but without taking away their control authority. Crucially, in this approach the force rendered to the user is not directly reflected in the motion of the robot (which is still directly controlled by the user); however, previous work in the area neglected to consider the possible instabilities in feedback loop generated by a user that over-responds to the haptic force. In this paper we introduce a differential constraint on the rendered force that makes the system finite-gain \mathcal{L}_2 stable; the constraint results in a Quadratically Constrained Quadratic Program (QCQP), for which we provide a closed-form solution. Our constraint is related to, but less restrictive than, the typical passivity constraint used in previous literature. We conducted an experimental simulation in which a human operator flies a UAV near an obstacle to evaluate the proposed method.

I. INTRODUCTION

Teleoperation allows human operators to remotely work in hard-to-reach or hazardous environments. When teleoperating an unmanned aerial vehicle (UAV), the typically limited field of view often leads to low levels of situational awareness, which can make it difficult to safely and accurately control the UAV [1], [2]. To remedy these challenges, there mainly exist two orthogonal approaches. The first one is shared autonomy, where a supervisory controller modifies the inputs of the user to guarantee safety [2]–[4]; these systems, however, reduce the control authority of the user. The second approach is shared control, where haptic signals provide force feedback cues about the robot’s behavior and the surrounding environment; this approach has shown reductions of dangerous collisions during teleoperation, and improvements in operator situational awareness. However, these works mostly focus on improving safety, without considering the fact that the human operator will likely change the commanded input in response to the haptic cues, thus resulting in a closed feedback loop. Only few works considered the stability of the full human-robot-environment system [5]–[7]. In this paper, we propose a novel shared control approach that considers not only the safety of the system, but also its overall stability while computing the force feedback.

¹Dawei Zhang is with the Department of Mechanical Engineering, Boston University, Boston, MA 02215, USA dwzhang@bu.edu.

²Roberto Tron is with the Department of Mechanical Engineering and the Division of Systems Engineering, Boston University, Boston, MA 02215, USA tron@bu.edu. He was partially supported by the NSF grant CMMI-1728277.

A. Related work

In this section, we review previous work that designs force-based haptic feedback to help human operators navigate a robot. We briefly mention their main characteristics, contrasting the novelty of our work in the next section.

Many researchers investigated algorithms about haptic feedback design. Haptic feedback that warns risk of collision is particularly relevant to the teleoperation of UAVs [2], [4], [8]. Lam et al. proposed a parametric risk field (PRF) to calculate the risk of a collision [8]. Brant and Colton set the magnitude of the force of the haptic feedback to be proportional to the time that it would take the UAV to collide with obstacles [2]. Recently, Zhang et al. designed an approach that uses control barrier functions (CBF) to generate haptic feedback that is based on the disagreement between the human’s control input and the safe control input calculated by Control Barrier Functions [4]. However, these works mostly focus on the algorithmic design of the haptic feedback and lack a stability analysis of the teleoperation system that considers the feedback loop through the user.

In this direction, Rifaï et al. [6] used Lyapunov analysis to prove the input-to-state stability of the teleoperation loop. Similar to [6], Omari et al. proved that the master system is input-to-state stable in the presence of bounded operator force and environment force [9]. Most of the stability analysis has the assumption that the human operator will navigate the robot passively, and that the environment is dissipative [10].

Since passivity provides a sufficient condition for stability, making the system passive is an intuitive method to maintain the stability of a teleoperation system [11]. Lee et al. proposed a Passive-Set-Position-Modulation (PSPM) method that modulates the set-position signal to enforce the passivity of the system and applied PSPM to the haptic teleoperation of multiple UAVs to make the system passive over the Internet with varying-delay, packet-loss [12], [13].

B. Proposed system and contributions

In this paper, we consider a teleoperation architecture of the form shown in Fig. 1. The *human* operator provides a desired velocity signal x_{2d} for a robot (quadrotor, in our case) through a *haptic device*. This desired velocity signal is given to a simple proportional velocity *controller* that generates a reference control signal u_{ref} which in turn is given to the actual *robot*. The *haptics generator* uses the state (position and velocity) of the robot to first compute a reference force F_{ref} via a Control Barrier Function method, then passing a safe projected version F which is rendered to the user via the

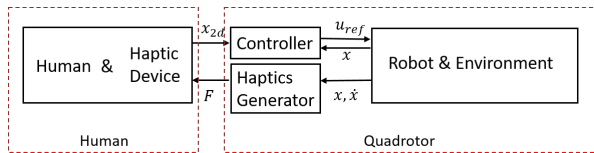


Fig. 1: Architecture of a haptic teleoperation system.

haptic device. Note that the human and quadrotor subsystems form a closed-loop interconnection.

The key contribution of this paper lies in the design of a differential constraint that enforces an arbitrarily small finite \mathcal{L}_2 gain from the user’s input to the rendered force. When coupled with the assumption that the user is also passive, the small gain theorem guarantees closed-loop stability. Our formulation has the following advantages:

- The \mathcal{L}_2 -gain differential constraint leads to a Quadratically Constrained Quadratic Program (QCQP), for which we provide a simple closed-form solution.
- Our method can be interpreted as a dynamic thresholding scheme that projects a desired reference force feedback to levels that are deemed to be safe (in the sense that they respect a desired \mathcal{L}_2 gain).
- Our approach does not assume that the force from the environment is passive, and can be applied to any scheme for generating the reference force. In this paper, we use the Control Barrier Functions method from [4].
- The new-designed differential constraint is less conservative than a similar strict output-passivity constraint, and allows the tracking of the desired reference force.

II. PRELIMINARIES

We first formally state the problem and review several control theory concepts used in the remainder of the paper.

A. Stability of teleoperation as a feedback interconnection

We view the teleoperation architecture of Fig. 1 as a feedback connection of two subsystems, *Human* and *Quadrotor*, as shown in Fig. 2. This interconnection is subject to two exogenous inputs: *Human intention*, representing the intentions of the operator (the desired motion), and *Disturbance*, representing physical disturbances on the robot, such as gusts of wind or minor collisions.

The goals of this paper are to design a force feedback scheme that ensures stability but that is also meaningful for the user, as formalized by the following two goals.

Goal 1: Design a *haptic generator* map that guarantees bounded state trajectories of the system under bounded *Human intention* and *Disturbance* inputs and under suitable assumptions on the *human* subsystem.

Goal 2: Design a *haptic generator* which produces a force feedback F with the following characteristics:

- (C1) If the quadrotor is far away from obstacles, or if the quadrotor is stationary, then $F = 0$.
- (C2) The force is approximately proportional to the distance and the velocity of the quadrotor in the direction of the obstacle (the faster and the closer the quadrotor, the higher the expected force). If the robot is moving away from an obstacle, no force should be generated.

(C3) For bounded inputs, the total amount of force received by the user should be bounded approximately proportional to the inputs (i.e., “small” commands should produce “small” forces).

(C4) Related to (C3), the output bounds should be applied over the entire trajectory, not independently at every time instant (in other words, the haptic generator should have some form of memory).

B. Control Barrier Functions (CBFs)

Following [4], we will use Control Barrier Functions to generate the reference haptic force feedback signal.

1) *State Space Model:* Consider a dynamical system represented by the state space model

$$\begin{aligned}\dot{\mathbf{x}} &= f(\mathbf{x}) + g(\mathbf{x})\mathbf{u} \\ \mathbf{y} &= c(\mathbf{x})\end{aligned}\quad (1)$$

where $\mathbf{x} \in \mathbb{R}^n$ is the state of the system, $\mathbf{u} \in \mathbb{R}^p$, $\mathbf{y} \in \mathbb{R}$ represent the vector of control inputs and the output, and $f: \mathbb{R}^n \rightarrow \mathbb{R}^n$, $g: \mathbb{R}^n \rightarrow \mathbb{R}^n \times \mathbb{R}^p$, and $c: \mathbb{R}^n \rightarrow \mathbb{R}$ are locally Lipschitz vector fields.

2) *Lie derivatives:* We denote the Lie derivative of a function $h(\mathbf{x})$ along a field $f(\mathbf{x})$ as $L_f h(\mathbf{x}) \doteq \frac{\partial h(\mathbf{x}(t))}{\partial \mathbf{x}(t)} \mathbf{f}(\mathbf{x})$. We denote with $L_f^b h(\mathbf{x})$ a Lie derivative of order b . The function h has relative degree 2 with respect to the dynamics (1) if $L_g h = 0$, and $L_g L_f h$ is a non-singular matrix. In this case we have $\dot{h} = L_f^2 h(\mathbf{x}) + L_g L_f h(\mathbf{x})\mathbf{u}$.

3) *Safety Set:* A continuously differentiable function $h(\mathbf{x})$ can define a safety set \mathcal{H} , as follows:

$$\mathcal{H} := \{\mathbf{x} \in \mathbb{R}^n : h(\mathbf{x}) \geq 0\}. \quad (2)$$

4) *CBFs for Second Order Systems:* The goal of control barrier functions is to produce a control field \mathbf{u} that makes a *safe set* $\mathcal{H} \subset \mathbb{R}^n$ forward invariant, i.e., so that if $\mathbf{x}(0) \in \mathcal{H}$ then $\mathbf{x}(t) \in \mathcal{H}, \forall t > 0$ [14]. Let $h(\mathbf{x})$ be a twice differentiable function representing \mathcal{H} , i.e. $h(\mathbf{x}) > 0$ on the interior of \mathcal{H} , $h(\mathbf{x}) = 0$ on its boundary, and $h(\mathbf{x}) < 0$ otherwise. Assuming that $h(\mathbf{x})$ has relative degree two, we can use a second-order exponential control barrier function [15] to impose constraints on \mathbf{u} that ensure safety (i.e., forward invariance of \mathcal{H}):

$$L_f^2 h(\mathbf{x}) + L_g L_f h(\mathbf{x})\mathbf{u} + K [h(\mathbf{x}) \quad L_f h(\mathbf{x})]^T \geq 0, \quad (3)$$

where $K \in \mathbb{R}^{1 \times 2}$ is a set of coefficients representing a Hurwitz polynomial.

C. \mathcal{L}_2 gain and feedback interconnections

In this section we review concepts that will be at the center of our solution to Goal 1. A map $\mathcal{C}: \mathbf{u}(t) \rightarrow \mathbf{y}(t)$ between two signals has \mathcal{L}_2 -gain $k \geq 0$ if there exists a constant $\beta \in \mathbb{R}$ such that $\|\mathbf{y}\|_2 \leq k\|\mathbf{u}\|_2 + \beta$. Note that the map \mathcal{C} could be static (i.e., a simple function) or, more commonly, realized through a dynamical system.

The importance of this concept is given by the *small gain theorem* (reproduced below in a slightly less generalized form specialized to our setting):

Theorem 1 (Theorem 5.6, page 218, [16]): Assume that both systems are finite-gain \mathcal{L}_2 stable with \mathcal{L}_2 gains of k_1

and k_2 : $\|\mathbf{u}\|_2 \leq k_1\|\mathbf{e}_1\|_2 + \beta_1$ and $\|\mathbf{F}\|_2 \leq k_2\|\mathbf{e}_2\|_2 + \beta_2$. If $k_1k_2 < 1$, then the feedback connection is finite-gain \mathcal{L}_2 stable from the inputs (*Human Intention*, *Disturbance*) to the outputs (\mathbf{e}_1 , \mathbf{e}_2).

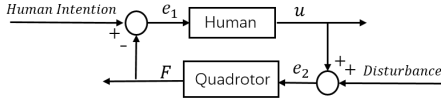


Fig. 2: Feedback connection.

As it is common in the literature, we assume that the human's reactions to the force feedback correspond to a map with a finite \mathcal{L}_2 gain.

D. Passivity

Although our final stability result will be based on the small gain theorem, passivity has been used to provide similar guarantees in previous work [6], [12]. We review the concept here for completeness; in Section III below we show that although one could use passivity to derive stability conditions similar to ours, these are significantly more restrictive and do not fulfill the characteristics listed in Goal 2.

Definition 1: The system in equation (1) is said to be *strictly output passive* if there exist a continuously differentiable positive semidefinite function $V(\mathbf{x})$ (called the storage function) and a static function $\rho(\mathbf{y})$ such that

$$\mathbf{u}^T \mathbf{y} \geq \dot{V} + k\mathbf{y}^T \rho(\mathbf{y}) \quad (4)$$

for all $(\mathbf{x}, \mathbf{u}) \in \mathbb{R}^n \times \mathbb{R}^p$, and $\mathbf{y}^T \rho(\mathbf{y}) > 0$ for all $\mathbf{y} \neq 0$. Intuitively, the storage function represents the amount of energy in the system, and passivity states that an increase (or decrease) in the energy is upper bounded by the work $\mathbf{u}^T \mathbf{y}$ that is possible to instantaneously transfer to (or extract from) the system. A typical choice for the function ρ is $\rho(\mathbf{y}) = \mathbf{y}$, which allows to connect passivity to \mathcal{L}_2 -gain theory:

Lemma 1 (Lemma 6.5, page 242, [16]): If the system 1 is output strictly passive with $\mathbf{u}^T \mathbf{y} \geq \dot{V} + k\mathbf{y}^T \mathbf{y}$, for some $k > 0$, then its \mathcal{L}_2 gain is less than or equal to k^{-1} .

In our setting, this means that the mechanical energy that the user receives from the system will be limited by the energy of the input they provide divided by k .

E. Quadrotor dynamic model

We consider a quadrotor that flies at relatively low speeds without highly aggressive maneuvers (which are exceedingly uncommon in a teleoperation setting), so that the roll and pitch angles of the quadrotor will remain small. Therefore, the dynamics of the UAV can be modeled by a double integrator, where the control input \mathbf{u} corresponds to the acceleration command of the UAV. Let $\mathbf{x} = \begin{bmatrix} \mathbf{x}_1 \\ \mathbf{x}_2 \end{bmatrix}$ be the state of the quadrotor, where \mathbf{x}_1 represents its position and $\mathbf{x}_2 = \dot{\mathbf{x}}_1$ its velocity. The dynamics of the system can be written as:

$$\begin{bmatrix} \dot{\mathbf{x}}_1 \\ \dot{\mathbf{x}}_2 \end{bmatrix} = \begin{bmatrix} 0 & I \\ 0 & 0 \end{bmatrix} \begin{bmatrix} \mathbf{x}_1 \\ \mathbf{x}_2 \end{bmatrix} + \begin{bmatrix} 0 \\ I \end{bmatrix} \mathbf{u}, \quad (5)$$

or, equivalently in matrix form:

$$\dot{\mathbf{x}} = \mathbf{A}\mathbf{x} + \mathbf{B}\mathbf{u}. \quad (6)$$

III. METHODS

To achieve Goal 1 and Goal 2, we propose to design a three-steps haptic generator:

- 1) Design a reference control input u_{ref} that is based on the human user's control input u .
- 2) Generate a reference force F_{ref} that guides the human user towards an input command that would be applied by a CBF-based collision-free controller.
- 3) Compute a force F that is as close as possible to F_{ref} , but satisfies the characteristics in Goal 1 and Goal 2.

The rest of this section illustrates the details of each step of the force feedback design. For Step 3) we first discuss an alternative differential constraint based on passivity (Section III-C), before proposing our solution based on finite \mathcal{L}_2 gain (Section III-D).

A. Reference controller

We define a simple reference proportional controller as

$$\mathbf{u}_{\text{ref}} = \frac{1}{\Delta_t}(\mathbf{x}_{2d} - B^T \mathbf{x}) = \frac{1}{\Delta_t}(\mathbf{x}_{2d} - \mathbf{x}_2), \quad (7)$$

where \mathbf{x}_{2d} is the input velocity set by the user, $B^T \mathbf{x} = \mathbf{x}_2$ is the current velocity of the robot, and Δ_t is a time constant representing for how long \mathbf{u}_{ref} will be applied to the robot (i.e., \mathbf{x}_2 will become \mathbf{x}_{2d} after Δ_t , i.e., in a single step).

The dynamics of the quadrotor subsystem then becomes:

$$\dot{\mathbf{x}} = \mathbf{A}\mathbf{x} + \mathbf{B}\mathbf{u}_{\text{ref}} = \left(\mathbf{A} - \frac{1}{\Delta_t}\mathbf{B}\mathbf{B}^T\right)\mathbf{x} + \frac{1}{\Delta_t}\mathbf{B}\mathbf{x}_{2d}. \quad (8)$$

We can rewrite the dynamics as:

$$\dot{\mathbf{x}} = \mathbf{A}_{\text{new}}\mathbf{x} + \mathbf{B}_{\text{new}}\mathbf{x}_{2d}, \quad (9)$$

where $\mathbf{A}_{\text{new}} = \begin{bmatrix} 0 & I \\ 0 & -\frac{1}{\Delta_t}I \end{bmatrix}$ and $\mathbf{B}_{\text{new}} = \begin{bmatrix} 0 \\ \frac{1}{\Delta_t}I \end{bmatrix}$.

B. Reference force

We design the reference force in two steps as done in [4]. First, we compute the safe input u_{CBF} that a CBF controller would provide for obstacle avoidance; then we design a reference force F_{ref} that depends on the discrepancy between u_{ref} and u_{CBF} . For the safe control input u_{CBF} we apply the material reviewed in Section II-B:

$$\begin{aligned} \mathbf{u}_{\text{CBF}} &= \underset{\mathbf{u} \in \mathbb{R}^m}{\text{argmin}} \frac{1}{2} \|\mathbf{u} - \mathbf{u}_{\text{ref}}\|^2 \\ \text{s.t. } & L_f^2 h(\mathbf{x}) + L_g L_f h(\mathbf{x})\mathbf{u} + K [h(\mathbf{x}) \quad L_f h(\mathbf{x})]^T \geq 0. \end{aligned} \quad (10)$$

where $f = \mathbf{A}\mathbf{x}$ and $g = \mathbf{B}$ are given by the original double integrator dynamics (5).

Then, we define the reference force \mathbf{F}_{ref} as:

$$\mathbf{F}_{\text{ref}} = \mathbf{u}_{\text{CBF}} - \mathbf{u}_{\text{ref}}. \quad (11)$$

C. Rendered force via passivity

Here we derive a differential constraint for designing the force F based on strict output passivity. As shown in the experiments (Section IV) this approach gives inferior results, but it has been used in previous literature and represents a convenient stepping stone for explaining our approach.

1) *Energy design*: We first identify the storage function

$$V(\mathbf{x}) = \frac{k_v}{2} \|B\mathbf{x}\|^2 = \frac{k_v}{2} \|\mathbf{x}_2\|^2, \quad (12)$$

where k_v is a constant parameter that adjusts the scale of the stored energy.

2) *Differential constraints*: We can find \mathbf{F} by looking for the force that is closest to \mathbf{F}_{ref} while satisfying the output passivity constraint:

$$\begin{aligned} \underset{\mathbf{F} \in \mathbb{R}^m}{\operatorname{argmin}} \quad & \frac{1}{2} \|\mathbf{F} - \mathbf{F}_{\text{ref}}\|^2 \\ \text{s.t.} \quad & \mathbf{x}_{2d}^T \mathbf{F} \geq \dot{V} + k\mathbf{F}^T \mathbf{F}, \end{aligned} \quad (13)$$

where we used the substitutions $\mathbf{u} = \mathbf{x}_{2d}$, $\mathbf{y} = \mathbf{F}$ in the strict output passivity constraint (4).

3) *Stability*: Following Lemma 6.5 of Khalil, the derivative of V satisfies

$$\begin{aligned} \dot{V} &\leq \mathbf{u}^T \mathbf{F} - k\mathbf{F}^T \mathbf{F} = \\ & - \frac{1}{2k} (\mathbf{u} - k\mathbf{F})^T (\mathbf{u} - k\mathbf{F}) + \frac{1}{2k} \mathbf{u}^T \mathbf{u} - \frac{k}{2} \mathbf{F}^T \mathbf{F} \\ & \leq \frac{1}{2k} \|\mathbf{u}\|^2 - \frac{k}{2} \|\mathbf{F}\|^2. \end{aligned} \quad (14)$$

which implies

$$\frac{k}{2} \|\mathbf{F}\|^2 \leq \frac{1}{2k} \|\mathbf{u}\|^2 - \dot{V} \quad (15)$$

Integrating both sides we have

$$\begin{aligned} \int_0^\tau \|\mathbf{F}\|^2 dt &\leq \frac{1}{k^2} \int_0^\tau \|\mathbf{u}\|^2 dt - \frac{2}{k} \int_0^\tau \dot{V} dt \\ &= \frac{1}{k^2} \int_0^\tau \|\mathbf{u}\|^2 dt + \frac{2}{k} (V(0) - V(\tau)) \\ &\leq \frac{1}{k^2} \int_0^\tau \|\mathbf{u}\|^2 dt + \frac{2}{k} V(0) \end{aligned} \quad (16)$$

This shows that the quadrotor subsystem has \mathcal{L}_2 gain equal to k^{-2} .

4) *Computational considerations*: Problem (13) is a convex Quadratically Constrained Quadratic program, which, however, has a simple close form solution. To derive such solution, we use the quadrotor dynamics (9) to expand $\dot{V} = k_v \mathbf{x}_2^T (\mathbf{x}_{2d} - \mathbf{x}_2)$, and then we rewrite the constraint (13) by completing the square:

$$\left\| \mathbf{F} - \frac{\mathbf{x}_{2d}}{2k} \right\|^2 \leq \left\| \frac{\mathbf{x}_{2d}}{2k} \right\|^2 - \frac{k_v}{k} \mathbf{x}_2^T \frac{1}{\Delta_t} (\mathbf{x}_{2d} - \mathbf{x}_2), \quad (17)$$

$$\left\| \mathbf{F} - \frac{\mathbf{x}_{2d}}{2k} \right\|^2 \leq \frac{1}{4k^2} (\mathbf{x}_{2d}^T \mathbf{x}_{2d} - \frac{4kk_v}{\Delta_t} \mathbf{x}_2^T \mathbf{x}_{2d} + \frac{4kk_v}{\Delta_t} \mathbf{x}_2^T \mathbf{x}_2). \quad (18)$$

Requiring that the discriminant of the quadratic polynomial in the RHS of (18) to be negative, we obtain that the constraint has a non-empty feasible region (i.e., positive RHS) under the condition that $0 \leq \frac{kk_v}{\Delta_t} \leq 1$.

With the constraint written in this form, we see that the QCQP problem (13) corresponds to a projection of \mathbf{F}_{ref} on the sphere centered at $\frac{1}{2k} \mathbf{x}_{2d}$ with radius given by the RHS of (18), which can be solved with simple geometrical considerations.

Remark 1: The closed-form solution highlights the main drawback of this passivity-based constraint: if the radius of the sphere is small, \mathbf{F} will be tied to be close to $\frac{\mathbf{x}_{2d}}{2k}$, independently from \mathbf{F}_{ref} .

D. Rendered force via finite gain

In this section we define a novel differential constraint that ensures a finite \mathcal{L}_2 gain for the quadrotor subsystem. The intuition behind our main contribution is that strict output passivity is a sufficient but not necessary condition for a finite \mathcal{L}_2 gain. This can be seen from the fact that the inequality in (14) is, in general, not tight; instead, we directly start from (15), but we also introduce an energy tank to dynamically balance the two sides of the equation, as described next.

1) *Energy design*: For our approach, we use the same storage function $V(\mathbf{x})$ from (12) that we used in the previous section. In addition, in order to make the constraint less restrictive, we introduce an energy tank E that is used to store energy when the reference force naturally satisfies (15), and releases energy when the reference force violates that same constraint. Formally, we view E as another state in the system, with dynamics

$$\dot{E} = \varepsilon. \quad (19)$$

Note that we could also add a tank to the passivity-based approach from the previous section; nonetheless, in subsection III-D.5 we show that even if we impose $E(0) \equiv 0$ (i.e., the tank cannot store or release energy) to make our approach comparable to the passivity-based method of Section III-C, our approach is still superior in terms of performance, as shown in the experiments in Section IV.

2) *Differential constraints*: We formulate a new force synthesis problem:

$$\min_{\mathbf{F}, \varepsilon} \frac{1}{2} \|\mathbf{F} - \mathbf{F}_{\text{ref}}\|^2 \quad (20a)$$

$$\text{subject to } \frac{k}{2} \|\mathbf{F}\|^2 + \varepsilon = \frac{1}{2k} \|\mathbf{u}\|^2 - \dot{V}, \quad (20b)$$

$$\varepsilon \geq -\frac{E}{\Delta_t} \quad (20c)$$

where (20b) is obtained by using the tank to balance (15), and where (20c) imposes the fact that the energy tank cannot be depleted too fast (namely, in less than one time step Δ_t). Additionally, note that (20c) also implies the constraint

$$\varepsilon \geq 0 \text{ if } E = 0. \quad (21)$$

3) *Stability*: Assuming $E(0) = 0$ and integrating both sides of the constraint (20b) we have

$$\begin{aligned} \int_0^\tau \|\mathbf{F}\|^2 dt + \int_0^\tau \dot{E} dt &= \int_0^\tau \|\mathbf{F}\|^2 dt + E(\tau) \\ &\leq \frac{1}{k^2} \int_0^\tau \|\mathbf{u}\|^2 dt + \frac{2}{k} V(0) \end{aligned} \quad (22)$$

which can be also rewritten as

$$\int_0^\tau \|\mathbf{F}\|^2 dt \leq \frac{1}{k^2} \int_0^\tau \|\mathbf{u}\|^2 dt + \frac{2}{k} V(0) - E(\tau) \quad (23)$$

Condition (21) implies $\int_0^\tau E dt = E(\tau) \geq 0$, which, together with (24), implies

$$\int_0^\tau \|\mathbf{F}\|^2 dt \leq \frac{1}{k^2} \int_0^t \|\mathbf{u}\|^2 dt + \frac{2}{k} V(0), \quad (24)$$

which guarantees that the quadrotor subsystem has finite \mathcal{L}_2 gain.

4) *Computational considerations:* Again, problem (20) is a convex QCQP. To find a closed-form solution, we obtain ε from the equality constraint in (20), and rewrite the optimization problem as

$$\begin{aligned} & \min_{\mathbf{F}, \varepsilon} \frac{1}{2} \|\mathbf{F} - \mathbf{F}_{\text{ref}}\|^2 \\ & \text{subject to } \|\mathbf{F}\|^2 \leq \frac{2}{k} \left(\frac{E}{\Delta_t} + \frac{1}{2k} \|\mathbf{u}\|^2 - \dot{V} \right). \end{aligned} \quad (25)$$

We can equivalently write the constraint of (25) as

$$\|\mathbf{F}\|^2 \leq \frac{1}{k^2} \left(\frac{2kE}{\Delta_t} + \mathbf{x}_{2d}^\top \mathbf{x}_{2d} - \frac{2kk_v}{\Delta_t} \mathbf{x}_2^\top \mathbf{x}_{2d} + \frac{2kk_v}{\Delta_t} \mathbf{x}_2^\top \mathbf{x}_2 \right). \quad (26)$$

Similarly to the previous section, knowing that $E \geq 0$ and requiring that the discriminant of the quadratic form in the RHS to be negative, we obtain that the constraint has a non-empty feasible region (i.e., positive RHS) under the condition that $0 \leq \frac{kk_v}{\Delta_t} \leq 2$.

With the constraint written in this form, we see that the QCQP problem (25) corresponds to a projection of \mathbf{F}_{ref} on the sphere centered at the origin with radius given by the RHS of (26), which can be implemented with a simple thresholding on the norm of \mathbf{F}_{ref} .

5) *Tank energy limits and comparison with passivity:* In practice, if the energy in the tank becomes too large, the bound on the force \mathbf{F} could become practically meaningless. Hence, we impose a threshold E_{max} on the maximum energy of the tank, and modify (19) to

$$\dot{E} = \begin{cases} \epsilon & \text{if } E < E_{\text{max}}, \\ 0 & \text{otherwise.} \end{cases} \quad (27)$$

If we set $E_{\text{max}} = 0$, we essentially disable the energy tank; in this case the approach becomes directly comparable with the passivity-based approach. In both cases we obtain QCQP which can be solved by projections on spheres. Comparing the RHSs of (26) and (18), the radii of the two spheres are the same (up to a factor of 2 in the choice of the coefficients). The main difference is that in the passivity approach the sphere is centered around \mathbf{x}_{2d} , while in the proposed approach it is centered around the origin. As shown in the next section, the latter leads to a much more natural behavior.

IV. EXPERIMENTAL VALIDATION

In this section, the proposed approach is evaluated through an experimental simulation in which the human operator navigates a simulated quadrotor in a virtual environment.

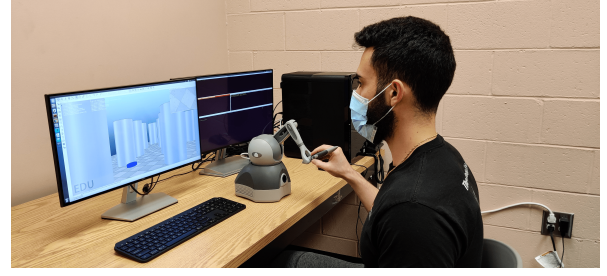


Fig. 3: A human operator uses a haptic joystick to control the UAV in a simulated environment with a first-person view.

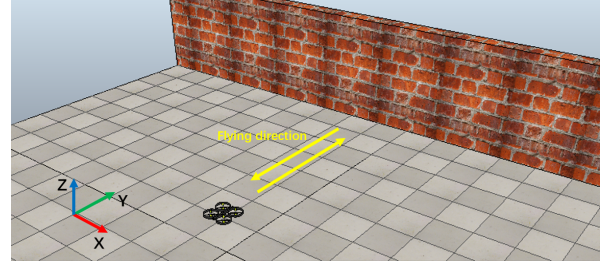


Fig. 4: A quadrotor UAV is navigated to approach a wall.

A. Experimental Setup

The UAV and the environment are simulated using CoppeliaSim [17]. As shown in Fig. 3, a 3D Systems Touch Haptic Device is used as the interface to control the motion of the UAV and provide haptic feedback to the operator. The communication between the haptic device and CoppeliaSim is performed via the Robot Operating System (ROS) middleware. The displacement of the stylus is mapped to the UAV's commanded velocity \mathbf{x}_{2d} through a constant of $0.2 \frac{m/s}{cm}$, with a dead-zone of 1 cm to help the user give a control command with zero velocity.

The experiment starts with navigating the UAV in a collision-free space. Then the human operator navigates the UAV towards and away from a vertical wall repeatedly for several times. During the experiment, we record the states of the UAV, the reference force feedback \mathbf{F}_{ref} , and the projected force feedback \mathbf{F} that is perceived by the human operator in the y-direction shown in Fig. 4.

As shown in Fig. 4, the obstacle in this experiment is a vertical wall that is 4 m away from the starting position of the UAV. Therefore, we pick the CBF in the form of

$$h(\mathbf{x}) = A_h^\top \mathbf{x}_1 + B_h, \quad (28)$$

where $A_h = \begin{bmatrix} 0 \\ -1 \end{bmatrix}$, $B_h = 4$. In this simulation, we set up Δ_t as 0.05 s and k_v in the storage function (12) as $\frac{\Delta_t}{2k} = \frac{0.025}{k}$.

B. Results and Discussion

We plot the results of the experiments projected on the y-axis coordinate in Fig. 5. As we can see from Fig. 5a and Fig. 5b, the force feedback that is provided to the human operator is zero when either the UAV flying away from the wall (e.g. from 11 s to 13 s) or the UAV staying stationary (e.g., 18 s to 20 s), which satisfies the proposed characteristic (C1). The CBF generates a reference force feedback F_{ref} as the UAV

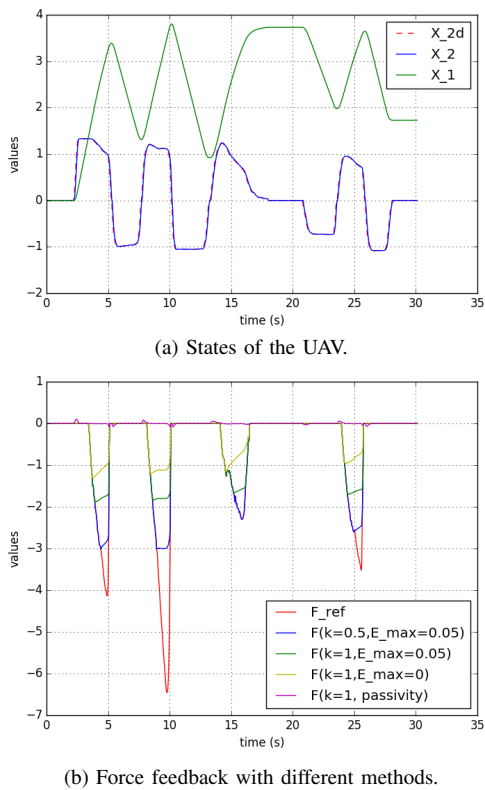


Fig. 5: Experimental results.

approaches the wall fast or gets close to the wall (e.g., from 8 s to 10 s) while the force feedback has the same trend with F_{ref} , which indicates that (C2) is satisfied. Furthermore, the value of the force feedback is bounded by the human's input with a \mathcal{L}_2 gain k , as depicted in Fig. 5b. A smaller value of k leads to a greater value of the force feedback. When the discrepancy between the human's control input and the CBF's safe input is too large, the bounded force feedback will keep the system finite-gain stable. This result is consistent with the characteristic (C3). As we can see from the result with condition ($k = 1, E_{\text{max}} = 0$) and condition ($k = 1, E_{\text{max}} = 0.05$), the bounds of the force feedback decrease over time (e.g., from 16 s to 17 s), which aligns well with the expected (C4). In addition, when applying the energy tank, the human operator receives a relatively higher value of the force feedback which depends on the upper limit, E_{max} , of the energy tank. As shown in Fig. 5b, when comparing the result under the condition ($k = 1, E_{\text{max}} = 0$) with the result under the condition ($k = 1, E_{\text{max}} = 0.05$), we can find that allowable force feedback can be increased by increasing E_{max} . Also, we can conclude that our approach with the energy tank is less conservative than the method without the energy tank and the method via strict output passivity. In particular, for the latter, considering Remark 1 and (18), one can see that when $\mathbf{x}_2 = \mathbf{x}_{2d}$, \mathbf{F} will be forced to be in the direction of \mathbf{x}_{2d} (which is opposite of \mathbf{F}_{ref}), thus leading to $\mathbf{F} = 0$ most of the time, while when $\mathbf{x}_2 \neq \mathbf{x}_{2d}$, $\mathbf{F} = 0$ is not a feasible solution, leading to the blips in Fig. 5.

V. CONCLUSIONS AND FUTURE WORK

In this paper, we proposed a novel haptic teleoperation approach that uses control barrier functions and small \mathcal{L}_2 gain to help the user maintain safety while also guaranteeing stability of the full system. We conducted an experimental simulation in which a human operator flies a UAV near an obstacle to evaluate the proposed method. The results show that the proposed approach behaves very similarly to a simple thresholding of the reference force generated by the CBF-based haptic method, and has very intuitive behavior.

In this work, we investigated our approach under the *haptic shared control* paradigm in which the human operator always keeps the control authority of the robot. In the future, we will further investigate our approach in a *haptic shared autonomy* paradigm where the human's control command to the robot is modified by CBF.

REFERENCES

- [1] J. S. McCarley and C. D. Wickens, "Human factors implications of uavs in the national airspace," Aviation Human Factors Division, Savoy, IL, Tech. Rep. AHFD-05-05/FAA-05-01, 2005.
- [2] A. M. Brandt and M. B. Colton, "Haptic collision avoidance for a remotely operated quadrotor UAV in indoor environments," in *IEEE Intl. Conf. on Systems Man and Cybernetics*, 2010, pp. 2724–2731.
- [3] X. Hou and R. Mahony, "Dynamic kinesthetic boundary for haptic teleoperation of aerial robotic vehicles," in *IEEE Intl. Conf. on Intelligent Robots and Systems*, 2013, pp. 4549–4950.
- [4] D. Zhang, G. Yang, and R. P. Khurshid, "Haptic teleoperation of uavs through control barrier functions," *IEEE Trans. on Haptics*, vol. 13, no. 1, pp. 109–115, 2020.
- [5] S. Stramigioli, R. Mahony, and P. Corke, "A novel approach to haptic tele-operation of aerial robot vehicles," in *IEEE Intl. Conf. on Robotics and Automation*, 2010, pp. 5302–5308.
- [6] H. Rifai, M.-D. Hua, T. Hamel, and P. Morin, "Haptic-based bilateral teleoperation of underactuated unmanned aerial vehicles," *IFAC Proceedings Volumes*, vol. 44, no. 1, pp. 13 782–13 788, 2011.
- [7] G. Gioioso, M. Mohammadi, A. Franchi, and D. Prattichizzo, "A force-based bilateral teleoperation framework for aerial robots in contact with the environment," in *IEEE Intl. Conf. on Robotics and Automation*, 2015, pp. 318–324.
- [8] T. M. Lam, H. W. Boschloo, M. Mulder, and M. M. Van Paassen, "Artificial force field for haptic feedback in UAV teleoperation," *IEEE Trans. on Systems, Man, and Cybernetics-Part A: Systems and Humans*, vol. 39, no. 6, pp. 1316–1330, 2009.
- [9] S. Omari, M.-D. Hua, G. Ducard, and T. Hamel, "Bilateral haptic teleoperation of VTOL UAVs," in *IEEE Intl. Conf. on Robotics and Automation*, 2013, pp. 2393–2399.
- [10] A. Y. Mersha, S. Stramigioli, and R. Carloni, "On bilateral teleoperation of aerial robots," *IEEE Trans. on Robotics*, vol. 30, no. 1, pp. 258–274, 2013.
- [11] G. Niemeyer, C. Preusche, and G. Hirzinger, "Telerobotics," in *Springer handbook of robotics*, 2008, pp. 741–757.
- [12] D. Lee and K. Huang, "Passive-set-position-modulation framework for interactive robotic systems," *IEEE Trans. on Robotics*, vol. 26, no. 2, pp. 354–369, 2010.
- [13] D. Lee, A. Franchi, P. R. Giordano, H. I. Son, and H. H. Bühlhoff, "Haptic teleoperation of multiple unmanned aerial vehicles over the internet," in *IEEE Intl. Conf. on Robotics and Automation*, 2011, pp. 1341–1347.
- [14] A. D. Ames, S. Coogan, M. Egerstedt, G. Notomista, K. Sreenath, and P. Tabuada, "Control barrier functions: Theory and applications," in *European Control Conference (ECC)*. IEEE, 2019, pp. 3420–3431.
- [15] Q. Nguyen and K. Sreenath, "Exponential control barrier functions for enforcing high relative-degree safety-critical constraints," in *American Control Conference (ACC)*. IEEE, 2016, pp. 322–328.
- [16] H. K. Khalil, *Nonlinear systems*. Prentice hall Upper Saddle River, 2002, vol. 3.
- [17] E. Rohmer, S. P. Singh, and M. Freese, "V-rep: A versatile and scalable robot simulation framework," in *IEEE/RSJ Intl. Conf. on Intelligent Robots and Systems*, 2013, pp. 1321–1326.